



Energy transfer process of anisothermal wall-bounded flows



Frédéric Aulery^{a,*}, Adrien Toutant^{a,b}, Françoise Bataille^{a,c}, Ye Zhou^d

^a PROMES CNRS – UPR 8521, Rambla de la Thermodynamique, Tecnosud, Perpignan, France

^b Université de Perpignan Via Domitia, 52 avenue Paul Alduy, 66860 Perpignan Cedex 9, France

^c Florida State University, Department of Mathematics, Tallahassee, FL, USA

^d Lawrence Livermore National Laboratory, Livermore, CA, USA

ARTICLE INFO

Article history:

Received 3 July 2014

Received in revised form 6 March 2015

Accepted 16 March 2015

Available online 18 March 2015

Communicated by F. Porcelli

ABSTRACT

Strong temperature gradients introduce a major external agency into the wall-bounded turbulent flows. In these flows, the temperature field and the turbulent velocity field are highly correlated. In fact, standard RANS turbulent models are not able to accurately reproduce these flows. In order to improve the performance of the models, we need to understand how the energy is produced, transferred, and dissipated in a strong anisothermal wall-bounded flow. This letter presents a first detailed investigation on the roles played by each contributor in the energy transfer equation.

© 2015 Elsevier B.V. All rights reserved.

1. Introduction

High Reynolds number turbulent flows in a wall bounded setting have many important scientific and engineering applications (see for example, [1]). Understandably, almost all publications have focused on the isothermal turbulence. The strong anisothermal flows, however, have received very limited attention because of the significant complexity introduced by the high temperature gradient. There is an urgent need to fill this gap since the anisothermal channel flows are directly relevant to the design of the solar energy devices. This letter is an effort to improve our understanding on the basic physics aspects of wall-bounded anisothermal flows.

The detailed turbulent kinetic energy transfer processes are a fundamental information for both isotropic and wall bounded turbulent flows. The dynamic equation for the energy transfer process, constructed from the Navier–Stokes equations, requires the input of three-dimensional velocity flows. Obtaining such time-dependent fields is a major challenge for the laboratory experiments as well as for the closure theories. Indeed, while the laboratory experiments can be carried out in any setting, the data collection is often limited by the diagnostic methodologies. On the other hand, the closure theories can be used to inspect high Reynolds number flows for incompressible [2] and weakly-compressible [3] flows. Unfortunately, these closure theories are restricted to the homogeneous and isotropic turbulence.

This investigation will utilize the databases from thermal direct numerical simulations. This is a well-established procedure for studying the energy transfer process. Numerical simulations have demonstrated their capabilities in providing high quality data for studying the energy transfer process. The previous works on homogeneous, isotropic turbulence have confirmed Kolmogorov's assumptions on the locality of the energy transfer [4] and interacting scales [5,6]. More recently, Domaradzki et al. [7], Marati et al. [8], Bolotnov et al. [9], and Cimarelli et al. [10,11] have extended the energy transfer analysis into the isothermal wall bounded flows.

To the best knowledge of the authors, the energy transfer analysis has not been performed for anisothermal wall turbulent flows. The high gradient of the temperature field introduces some interesting new physics [12]. The local Reynolds numbers are significantly different at the hot and cold sides. Furthermore, it was found that the Kolmogorov scaling is no longer valid when the flow is submitted to strong dilatation caused by the temperature gradients [13]. This phenomenon is analogous to those turbulent flows subject to external agencies [14–16]. As a result, it is expected that the spectral energy analysis of the anisothermal flows should offer fresh insights on how the energy is moved about within the channel. This letter will provide detailed information on all-important components in the energy transfer process: the production, nonlinear transfer, and viscous effects terms.

The letter is organized as follows. The formulation of the physical problem will be discussed in the next section. The detailed energy transfer study can be found in Section 3. Finally, the conclusion is given in Section 4.

* Corresponding author.

E-mail addresses: frederic.aulery@gmail.com (F. Aulery), zhou3@llnl.gov (Y. Zhou).

2. Equations and numerical dataset

2.1. Governing equations

The thermal direct numerical simulations are based on the standard governing equations (see for example, [17]):

Mass conservation

$$\frac{\partial \rho}{\partial t} + \frac{\partial \rho U_i}{\partial x_i} = 0 \quad (1)$$

Momentum conservation

$$\frac{\partial \rho U_i}{\partial t} + \frac{\partial \rho U_i U_j}{\partial x_j} = -\frac{\partial P_{dyn}}{\partial x_i} + \frac{\partial}{\partial x_i} \left[\mu \left(\frac{\partial U_i}{\partial x_j} + \frac{\partial U_j}{\partial x_i} \right) \right] + \frac{2}{3} \frac{\partial}{\partial x_i} \left(\mu \frac{\partial U_j}{\partial x_j} \right) \quad (2)$$

Energy conservation

$$\frac{\partial C_p \rho T}{\partial t} + \frac{\partial C_p \rho T U_j}{\partial x_j} = -\frac{\partial P_{th}}{\partial t} + \frac{\partial}{\partial x_j} \left[\lambda \left(\frac{\partial T}{\partial x_j} \right) \right] \quad (3)$$

Ideal gas law

$$P_{th} = \rho r T \quad (4)$$

The thermodynamical pressure is constant in space

$$\frac{\partial P_{th}}{\partial x_i} = 0 \quad (5)$$

The transport coefficients are given by

$$\mu(T) = \mu_0 \left(\frac{T}{T_0} \right)^{3/2} \frac{T_0 + S}{T + S} \quad Pr = 0.7 = \frac{\mu C_p}{\lambda} \quad (6)$$

Here, the fluid viscosity follows the well-known Sutherland law and the conductivity is computed using the Prandtl number (Eq. (6)). In order to isolate the effects of the temperature gradient, we will restrict our attention to a low Mach number flow so that the pressure dilatation can be ignored. This assumption split the pressure into two parts. The main part, called the thermodynamical pressure, represents the compressibility part of the pressure. The dynamical pressure is the minor part and is linked to the momentum. The fluid material is air. The anisothermal flow is established by having the two plates with different temperatures at the bottom ($T_1 = 293$ K) and top ($T_2 = 586$ K) of the channel (Fig. 1). The distance between the two plates (L_y) equals to $2h$, where $h = 15$ mm. The other domain lengths (L_x and L_z), in the longitudinal and transversal directions, are equal to $4\pi h$ and $2\pi h$, respectively. It should be noted that the x and z coordinates are the periodic directions of the channel.

The governing equations are solved using the Trio_U software, which is a finite volume solver [18]. The velocity advective scheme is a centered fourth order one, and the scalar advective scheme is an upwind third order one. The flow rate is imposed to obtain a mean turbulent Reynolds number of $Re_\tau = 180$. The Reynolds number is given by $Re_\tau = \frac{U_\tau h}{\nu} = \frac{Re_\tau^{hot} + Re_\tau^{cold}}{2}$. Here U_τ is the mean friction velocity; Re_τ^{hot} and Re_τ^{cold} are the Reynolds numbers defined at the hot and cold walls. The mesh has $192 \times 140 \times 288$ cells with a first cell size $\Delta y^+ = 0.25$. The data collections are carried out during 5.657 s of the computation, which corresponds to 50 characteristic times of the hot side, $t_c = \frac{h}{U_\tau} = 0.11428$ s (t_c is greater at the hot side than that at the cold side). The sample time is equal to $0.01t_c$.

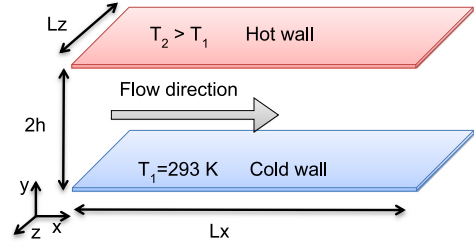


Fig. 1. Channel configuration.

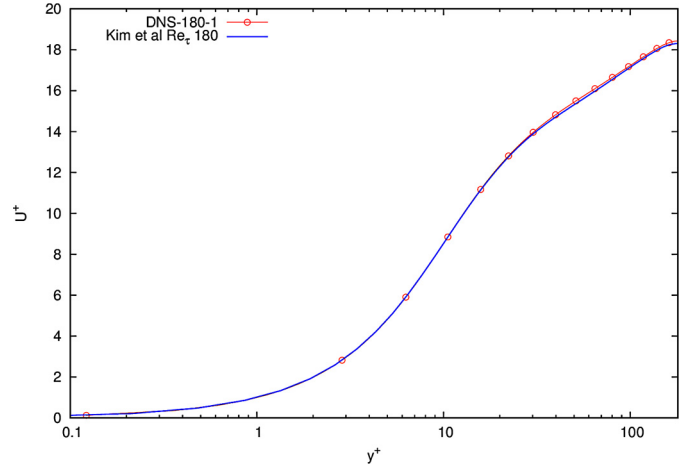


Fig. 2. Mean longitudinal velocity compared to Kim et al. [19].

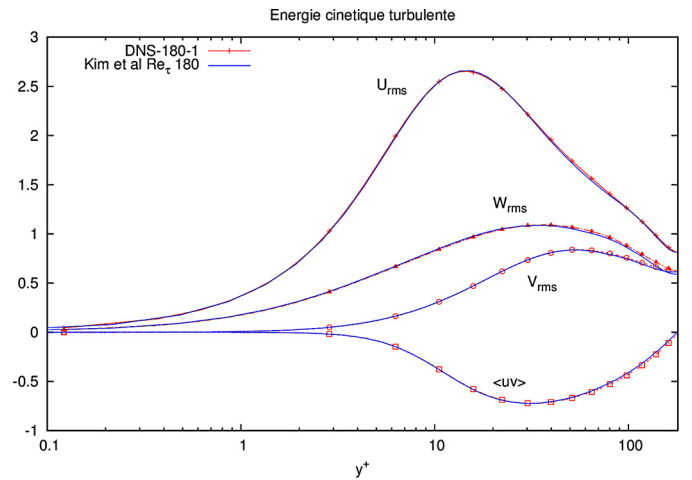


Fig. 3. Root mean square velocity fluctuations and velocity correlation compared with Kim et al. [19].

2.2. Numerical simulation validation at the isothermal limit

In this and next subsection, our numerical process will be validated. First of all, we performed a direct numerical simulation (DNS) of an isothermal channel flow at a turbulent flow with its Reynolds number $Re_\tau = 180$, which is the same condition of the flow previously computed by Kim et al. [19]. The comparisons between two simulations are presented in Figs. 2 and 3, where the results from current simulations are represented by dots and their counterparts from Kim et al. are denoted by lines. It is clear that the mean velocity profiles and root mean square velocity fluctuations are in excellent agreement. As a result, our numerical simulations are validated at the isothermal limit.

Download English Version:

<https://daneshyari.com/en/article/1860979>

Download Persian Version:

<https://daneshyari.com/article/1860979>

[Daneshyari.com](https://daneshyari.com)